Available online at www.sciencedirect.com
ScienceDirect
Journal of Catalysis 251 (2007) 354–362
JOURNAL OF CATALYSIS
www.elsevier.com/locate/jcat

# Synthesis and characterization of MoVTeCeO catalysts and their catalytic performance for selective oxidation of isobutane and isobutylene

Jingqi Guan, Shujie Wu, Hongsu Wang, Shubo Jing, Guojia Wang, Kaiji Zhen, Qiubin Kan *

*College of Chemistry, Jilin University, Changchun 130023, PR China*

Received 21 June 2007; revised 28 July 2007; accepted 31 July 2007

Available online 18 September 2007

**Abstract**

A series of Mo-based catalysts (MoVCeO, MoTeCeO, MoVTeO, and MoVTeCeO mixed metal oxides) were prepared and tested for the oxidation of isobutane and isobutylene. Characterization results (XRD, FTIR, TPR, XPS, and BET) showed that their structure and properties depend on the composition of the calcined samples. Catalytic tests showed that molybdenum may be the key element for the activation of isobutane, whereas the selective oxidation of isobutylene to methacrolein (MAL) might proceed mainly on the surface of the TeMo-containing crystalline phase. In addition, $Te^{4+}$ may favor the formation of methacrylic acid (MAA). The incorporation of Ce ions may modify the redox process of the catalysts and thus influence the catalytic behaviors for the selective oxidation of isobutane. Thus, the selectivities and yields of MAL and MAA can be increased over these specially designed catalysts.


*Keywords:* Isobutane; Isobutylene; Selective oxidative; Methacrolein; Methacrylic acid

## 1. Introduction

The one-step selective oxidation of isobutane to methacrolein (MAL) and methacrylic acid (MAA) is an attractive alternative to the conventional multistep catalytic oxidation reaction of acetone with hydrogen cyanide due to its simplicity, inexpensive raw materials, and negligible environmental impact. Thus reaction has been extensively studied for a long time worldwide [1–5]. Many catalytic systems have been investigated for the selective catalytic oxidation of isobutane [1–12].

Up to now, the most promising catalysts for the selective oxidation of isobutane to MAA are heteropolyacids and their polyoxometalate derivatives with Keggin structures [13–15]. It has been suggested that Mo-containing species should be the active sites [14], whereas the addition of some transition metals (e.g., V, Cu, Fe) can enhance the catalytic performance by promoting catalyst reoxidation. However, a problem encountered is the low thermal stability of the Keggin-type polyoxometalates, which begin to decompose at the temperature for the activation of alkane [16]. In addition, another important aspect of this reaction is that alkane-rich conditions have been widely used as feed materials [17]. However, under these conditions, the isobutane conversion is inevitably very low (in general, $\leqslant 25\%$); therefore, it is necessary to recycle the unconverted reactants.

In addition, the mixed metal oxides are very promising catalysts for the selective oxidation of isobutane to isobutylene and MAL [6–12]. Among these, Ce–Zr mixed oxides have been used for the selective oxidation of isobutane to isobutylene, and their catalytic performance has been reported to be relatively good [18]. The oxidative dehydrogenation reaction is improved due to the redox properties of $CeO_2$ and its ability to store and release oxygen under oxidation and reduction conditions, respectively.

But the most effective mixed-oxide catalysts for isobutane oxidation to MAL are Mo–V–Te–Sb–O catalysts, as reported by Guan et al. [11]. It has been suggested that in the Mo–V–Te–Sb–O system, the pseudohexagonal so-called "M1 phase" ($Te_{0.33}MO_3$; $M$ = Mo, V, and Sb) might favor selectivity to MAL. These authors also have reported that adding a small amount of antimony to the MoVTeP-based system produces a relative increase in the selectivity to MAL but decreased selectivity to $CO_x$ (CO and $CO_2$) [12]. The incorporation of Sb can

* Corresponding author.
*E-mail address:* qkan@mail.jlu.edu.cn (Q. Kan).

0021-9517/$ – see front matter 
doi:10.1016/j.jcat.2007.07.028

modify the active and selective sites for the transformation of isobutane to isobutylene and MAL, and slow the consecutive total combustion reactions of MAL to $CO_x$.

In this paper, we report on the introduction of Ce ions, which have a strong capability to transport oxygen to the MoVTe-based catalysts to facilitate the migration of lattice oxygen in the lattice. TPR results have shown that the reducibility of catalysts has been modified. Catalytic data indicate that incorporating a small amount of Ce increases the selectivities to MAL and MAA.

## 2. Experimental

### 2.1. Catalyst preparation

The MoVTeCeO catalysts were prepared as follows. First, ammonium metavanadate was dissolved in water at 80 °C under stirring, and then ammonium heptamolybdate and telluric acid were added into the metavanadate solution. Half an hour later, a different amount of cerous nitrate was added. The mixture was further stirred at 80 °C to remove volatiles. The resultant solid was dried at 110 °C overnight, and finally calcined in a flow of nitrogen at 600 °C for 2 h to obtain the final metal oxides. For comparison, MoVO, MoVTeO, MoVCeO, and MoTeCeO catalysts were also prepared under similar conditions.

### 2.2. Catalyst characterization

The specific surface areas of the catalysts were measured based on the adsorption isotherms of $N_2$ at −196 °C using the BET method (Micromeritics ASAP2010). Powder X-ray diffraction (XRD) patterns were collected using a Shimadzu XRD-6000 scanning at 4°/min with Cu$K\alpha$ radiation (40 kV, 30 mA). The infrared spectra (IR) of various samples were recorded at room temperature using a NICOLET Impact 410 spectrometer.

X-ray photoelectron spectra (XPS) were recorded on a VG ESCA LAB MK-II X-ray electron spectrometer using Al$K\alpha$ radiation (1486.6 eV, 10.1 kV). The spectra were referenced with respect to the C 1s line at 284.7 eV. The measurement error of the spectra was ±0.2 eV.

$H_2$-temperature programmed reduction (TPR) experiments were carried out in a flow reactor system, in which 10 mg of catalyst was charged each run into a U-shaped quartz microreactor (4 mm i.d.). After purging with Ar gas from 50 to 300 °C at a ramp rate of 10 °C/min, holding at 300 °C for 30 min, and cooling to 100 °C, the sample was reduced in a 5% $H_2$/Ar stream (25 ml/min). The reduction temperature was raised uniformly from 100 to 800 °C at a ramp of 10 °C/min. $H_2$ consumption was measured by a thermal conductivity detector (TCD).

### 2.3. Catalytic tests

The reaction was performed in a stainless steel tubular fixed bed reactor (16 mm i.d., 400 mm long) under atmospheric pressure. Each catalytic test was carried out using 1.0 g of catalyst, which was granulated into particles of 20–30 mesh size and diluted with 0.5 g of SiC particles to prevent temperature gradients and hot spots in the reactor. Under our reaction conditions, the homogeneous reaction can be neglected. Carbon balance was always >95%.

The feed was controlled by a mass flow controller, and water was fed by a mini-pump. The catalytic reaction condition was as follows: molar ratio of the feed gas $i$-$C_4H_{10}$:$O_2$:$N_2$:$H_2O$ = 1:2.5:2:2, $i$-$C_4H_8$:$O_2$:$N_2$:$H_2O$ = 1:6:6:6. The experiments were carried out at 420 °C. Gaseous products were analyzed by an online gas chromatograph with a GDX-501 column and a flame ionization detector (FID; Shimadzu GC-8A). Other products were analyzed by a gas chromatograph with a GDX-501 column containing an 8% polyethylene glycol sebacate/2% sebacic acid and an FID (Shimadzu GC-8A). Isobutylene ($i$-$C_4^=$), methacrolein (MAL), methacrylic acid (MAA), $CO_x$ (CO, $CO_2$), propylene ($C_3^=$), and acetic acid (HAC) were the main products. Small amounts of propane, acetone, acrolein, and acrylic acid also were detected.

## 3. Results and discussion

### 3.1. XRD studies

XRD patterns of the prepared catalysts are shown in Fig. 1. For the Te-free sample $MoV_{0.3}Ce_{0.2}$, the peaks at $2\theta$ = 22.1°, 23.7°, 26.2°, 29.7°, and 31.7° can be assigned to $(V_{0.07}Mo_{0.93})_5O_{14}$ [JCPDS 31-1437], whereas peaks at $2\theta$ = 14.7°, 22.6°, 24.6°, 29.1°, 32.9°, 39.1°, and 39.7° can be attributed to $Ce_2(MoO_4)_2(Mo_2O_7)$ [JCPDS 76-1040]. Moreover, peaks at $2\theta$ = 28.5°, 33.1°, 47.5°, and 59.1° can be assigned to $CeO_2$ [JCPDS 81-0792], and peaks at $2\theta$ = 12.8°, 23.7°, 25.9°, 27.3°, 33.7°, 39.1°, 39.7°, and 49.3° can be attributed to $MoO_3$ [JCPDS 35-0609]. In contrast, the XRD pattern of the V-free sample $MoTe_{0.23}Ce_{0.2}$ indicates the presence of $MoO_3$, $Ce_2(MoO_4)_2(Mo_2O_7)$, and $TeMo_5O_{16}$ ($2\theta$ = 21.8°, 24.6°, 26.6°, 27.3°, 30.5°, 31.0°, and 34.4°) [JCPDS 88-0407].

Meanwhile, the XRD pattern of the Ce-free sample $MoV_{0.3}Te_{0.23}$ indicates the presence of $MoO_3$, $(V_{0.07}Mo_{0.93})_5O_{14}$, Te-

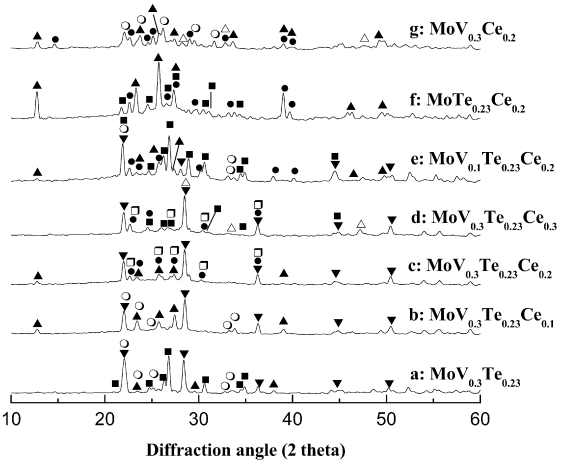


Fig. 1. XRD patterns of samples calcined at 600 °C in $N_2$: (▲) $MoO_3$, (△) $CeO_2$, (●) $Ce_2(MoO_4)_2(Mo_2O_7)$, (○) $(V_{0.07}Mo_{0.93})_5O_{14}$, (■) $TeMo_5O_{16}$, (□) $CeMo_2O_8$, (▼) TeMO (TeVMoO and/or TeVCeMoO) crystalline phase.

$Mo_5O_{16}$, and a new Te$MO$ ($M$ = Mo and V) crystalline phase ($2\theta = 22.1°$, 28.3°, 36.4°, 44.6°, and 50.2°), which could correspond to the hexagonal phase M1 ($Te_{0.33}MO_3$; $M$ = Mo, V, and Nb), as proposed by Aouine et al. [19–22]. When cerium was added into the MoVTe-based system at a Ce/Mo ratio of 0.1, the peaks corresponding to $TeMo_5O_{16}$ disappeared and the intensities of the peaks corresponding to $MoO_3$ increased. However, a further increase of cerium content to a Ce/Mo ratio of 0.2 caused the appearance of peaks at $2\theta = 22.6°$, 25.9°, 27.5°, 30.3°, and 36.4°, suggesting the presence of $CeMo_2O_8$ [JCPDS 32-0194], and the appearance of peaks at $2\theta = 22.6°$, 23.4°, 25.9°, 27.5°, 30.3°, and 36.4°, which can be attributed to $Ce_2(MoO_4)_2(Mo_2O_7)$ [JCPDS 76-1040]. However, the peaks corresponding to $(V_{0.07}Mo_{0.93})_5O_{14}$ disappeared. When cerium content was further increased to a Ce/Mo ratio of 0.3, a new phase $CeO_2$ could be observed, whereas the peaks corresponding to $MoO_3$ disappeared.

In addition, the XRD patterns of $MoV_{0.1}Te_{0.23}Ce_{0.2}$ (Fig. 1e) were relatively different from those of other MoVTeCeO samples, such as $MoV_{0.3}Te_{0.23}Ce_{0.2}$ (Fig. 1c), because the peak at $2\theta = 28.5°$ corresponding to Te$MO$ crystalline phase was shifted to 28.2° and its intensity decreased remarkably. This is because the decreased V content in the system may relatively reduce the content of the Te$MO$ phase. Botella et al. also reported similar results, demonstrating that the new Te$MO$ phase increased with increasing V content [20].

### 3.2. FTIR studies

The FTIR spectra of the prepared catalysts are shown in Fig. 2. For the Te-free sample $MoV_{0.3}Ce_{0.2}$ (Fig. 2g), the bands at 1012, 907, and 585 $cm^{-1}$ are probably related to V=O groups and V–O–Me (Me = Mo, V, and Ce) bonds [11,20], whereas the bands at 993, 878, and 820 $cm^{-1}$ can be attributed to $MoO_3$. In addition, bands at 500–900 $cm^{-1}$ (e.g., 845, 791, 759, 733, 631, and 557 $cm^{-1}$) are due to antisymmetric vibrations of Mo–O–Me bridging bonds [23–25].

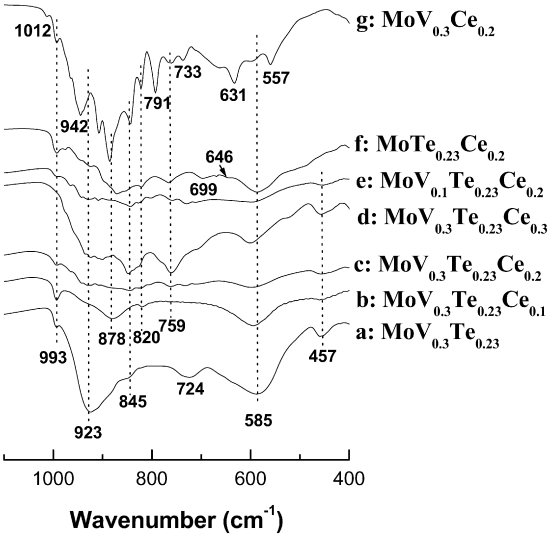


Fig. 2. FTIR spectra of samples calcined at 600 °C in $N_2$.

Similarly, for the V-free catalyst $MoTe_{0.23}Ce_{0.2}$ (Fig. 2f), it can be seen that the bands at 993, 870, and 820 $cm^{-1}$ are associated with the presence of $MoO_3$, whereas the bands at 852 $cm^{-1}$ are probably due to antisymmetric vibrations of Mo–O–Me (Me = Mo and Ce) bridging bonds. Moreover, the bands at 923, 820, 699, 646, and 585 $cm^{-1}$ with a shoulder at 765 $cm^{-1}$ can be attributed to $TeMo_5O_{16}$ [20]. However, Ce species could be partially incorporated into the $TeMo_5O_{16}$ structure and change the positions of the Mo–O bands (bands at 913, 800, 725, and 500 $cm^{-1}$) and Te–O bands (bands at 765 and 630 $cm^{-1}$) [20].

In the same way, the FTIR spectrum of Ce-free sample $MoV_{0.3}Te_{0.23}$ (Fig. 2a) shows a band at 993 $cm^{-1}$, which should be attributed to symmetric stretching vibration of Mo=O bonds in $MoO_3$, whereas the band detected at 845 $cm^{-1}$ is due to antisymmetric vibrations of Mo–O–Me (Me = Mo and V) bridging bonds. Furthermore, the bands at 923, 724, and 585 $cm^{-1}$ should be related to $TeMo_5O_{16}$ phase. All of these bands may have shifted from their original positions due to the incorporation of Ce atoms into the system. The incorporated Ce may have interacted with Mo atoms and thereby formed new Mo–O–Ce bands, which in return affected the growth of other Mo–O species. As a result, when cerium was added into the MoVTe-based system, the intensity of the band at 923 $cm^{-1}$ corresponding to Mo–O bond in the $TeMo_5O_{16}$ phase decreased dramatically. But the intensities of the bands corresponding to Mo–O–Ce increased gradually, especially of the band at 759 $cm^{-1}$. In addition, when the Ce/Mo ratio reached 0.3, the band at 993 $cm^{-1}$ disappeared.

Combined with the XRD results, these findings lead us to conclude that no $MoO_3$ crystallite exists in the $MoV_{0.3}Te_{0.23}Ce_{0.3}$ catalyst. The infrared spectra along with the XRD patterns indicate that in both cases, we have an intimate mixture of several phases, some of which are XRD-amorphous.

### 3.3. Specific surface area determination and XPS studies

Table 1 shows the specific surface area and XPS data of the catalysts. The catalysts' specific surface areas depended on their composition. In general, the initial incorporation of cerium into the Mo–V–Te-based system decreased the specific surface area, which began to increase slowly with increasing cerium content. Moreover, the V and Te content also affected the catalysts' surface area. The catalysts' surface composition strongly depended on the nominated amount of each element. No vanadium ions were detected on the catalyst surface when relatively low amounts of cerium were added into the $MoV_{0.3}Te_{0.23}Ce_x$ system. Only when relatively high content of cerium (Ce/Mo = 0.3) were added could vanadium ions be detected by XPS. In addition, the tellurium content increased when the cerium was initially added into the catalysts, whereas it decreased with further increases in cerium content. However, the cerium content on the surface of the $MoV_{0.3}Te_{0.23}Ce_{0.2}$ catalyst was the lowest among the samples tested.

To gain deeper insight into the surface constitution and properties of these catalysts, we investigated their binding energies (Mo $3d_{5/2}$, Te $3d_{5/2}$, V $2p_{3/2}$, and Ce $3d_{5/2}$). The corresponding

Table 1
BET surface area and XPS data of samples calcined at 600 °C in $N_2$

| Sample | $S_{BET}$ ($m^2\,g^{-1}$) | Surface composition | Binding energy (eV) | | | | Surface oxidation states | | | |
|---|---|---|---|---|---|---|---|---|---|---|
| | | Mo/V/Te/Ce | Mo $3d_{5/2}$ | V $2p_{3/2}$ | Te $3d_{5/2}$ | Ce $3d_{5/2}$ | $Mo^{6+}/Mo^{5+}$ | $V^{5+}/V^{4+}$ | $Te^{6+}/Te^{4+}$ | $Ce^{4+}/Ce^{3+}$ |
| $MoV_{0.3}Te_{0.23}$ | 3.0 | 1/0.06/0.13/0 | 232.9 | 516.5 | 576.2 | – | 0.62/0.38 | 0.25/0.75 | 0.23/0.77 | – |
| $MoV_{0.3}Te_{0.23}Ce_{0.1}$ | 1.7 | 1/0/0.17/0.08 | 232.9 | – | 576.2 | 881.6 | 0.63/0.37 | 0/0 | 0.23/0.77 | 0.68/0.32 |
| $MoV_{0.3}Te_{0.23}Ce_{0.2}$ | 2.1 | 1/0/0.11/0.03 | 232.9 | – | 576.3 | 882.8 | 0.86/0.14 | 0/0 | 0/1 | 0.61/0.39 |
| $MoV_{0.3}Te_{0.23}Ce_{0.3}$ | 2.6 | 1/0.1/0.08/0.1 | 232.8 | 516.5 | 576.1 | 882.6 | 0.95/0.05 | 0.59/0.41 | 0.12/0.88 | 0.56/0.44 |
| $MoV_{0.1}Te_{0.23}Ce_{0.2}$ | 0.8 | 1/0.06/0.41/0.08 | 232.8 | 517.9 | 577.2 | 885.1 | 0.65/0.35 | 0.75/0.25 | 0.84/0.16 | 0/1 |
| $MoTe_{0.23}Ce_{0.2}$ | 1.2 | 1/0/0.23/0.06 | 232.8 | – | 577.1 | 884.8 | 0.83/0.17 | – | 0.86/0.14 | 0.19/0.81 |
| $MoV_{0.3}Ce_{0.2}$ | 3.4 | 1/0.22/0/0.09 | 232.8 | 517.1 | – | 883.8–886.5 | 0.9/0.1 | 1/0 | – | 0.38/0.62 |

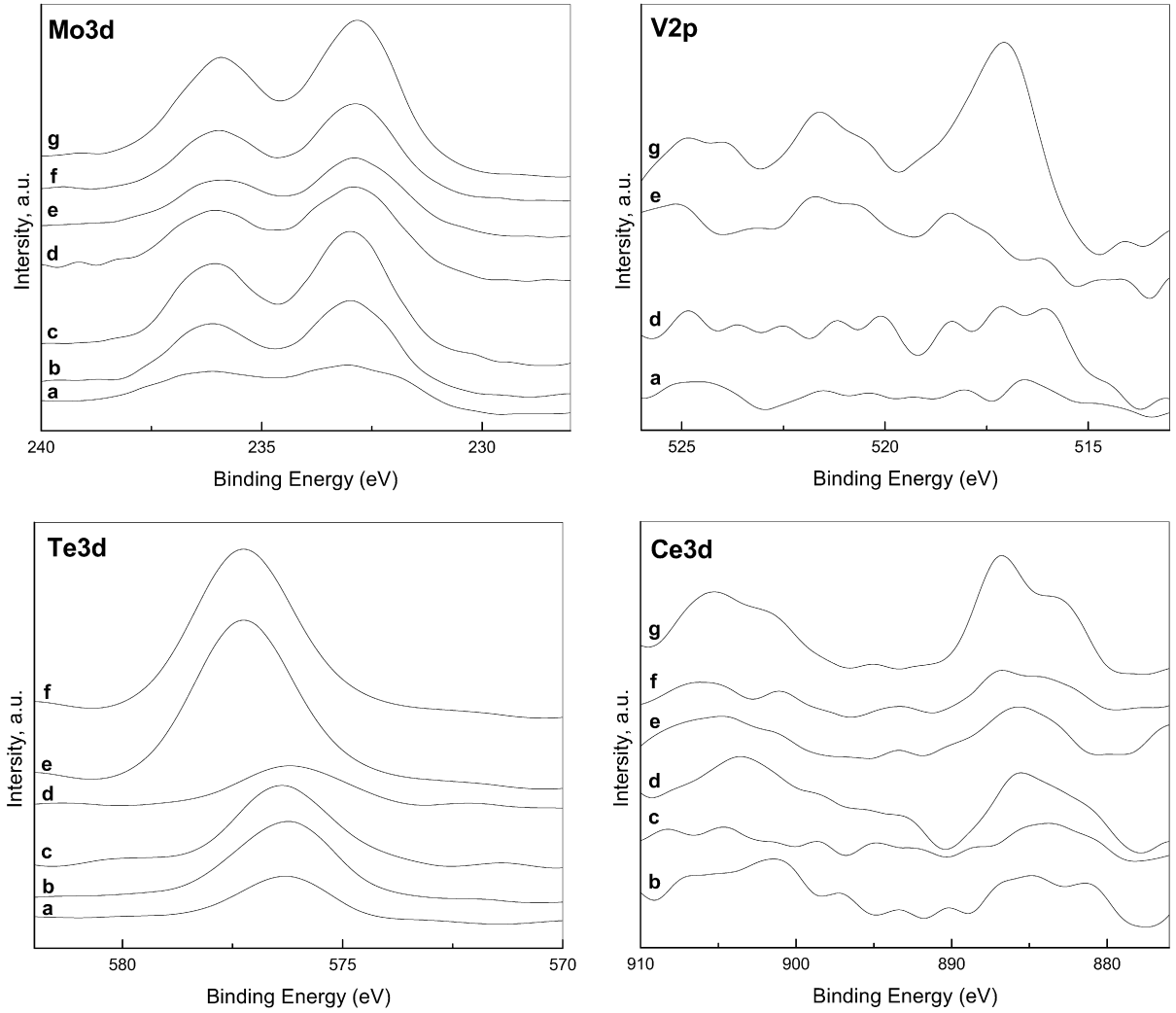


Fig. 3. X-ray photoelectron spectra corresponding to the main transitions (Mo $3d_{5/2}$, Te $3d_{5/2}$, V $2p_{3/2}$, and Ce $3d_{5/2}$) of calcined catalysts: (a) $MoV_{0.3}Te_{0.23}$, (b) $MoV_{0.3}Te_{0.23}Ce_{0.1}$, (c) $MoV_{0.3}Te_{0.23}Ce_{0.2}$, (d) $MoV_{0.3}Te_{0.23}Ce_{0.3}$, (e) $MoV_{0.1}Te_{0.23}Ce_{0.2}$, (f) $MoTe_{0.23}Ce_{0.2}$, (g) $MoV_{0.3}Ce_{0.2}$.

spectra are shown in Fig. 3, they are composed and integrated with the results shown in Table 1. The Mo $3d_{5/2}$ peak of the catalysts can be fitted mainly into two components at 231.7 and 232.8 eV, which can be related to $Mo^{5+}$ and $Mo^{6+}$, respectively [26,27]. However, the binding energy of Mo ions in a 4+ oxidation state (typical value of 230.9 eV in $MoO_2$) is not observed [28]. As shown in Fig. 3 and Table 1, the $Mo^{6+}/Mo^{5+}$ surface atomic ratios increased with increasing Ce content, suggesting that the coordinatively unsaturated $Mo^{5+}$ was pronely oxidized to $Mo^{6+}$ by $Ce^{4+}$.

The V $2p_{3/2}$ peak of catalysts could be fitted into two components at 516.2 and 517.3 eV, which can be related to $V^{4+}$ and $V^{5+}$ species, respectively [29]. A greater amount of $V^{5+}$ was present on the Ce-containing catalyst surface than on the Ce-free catalyst surface. In addition, the presence of $V^{4+}$ species in Te-containing samples, which was not observed in Te-free

sample, suggests that the presence of Te can favor the reduction of $V^{5+}$.

The Te $3d_{5/2}$ peak of catalysts could be fitted into two components at 576.2 and 577.3 eV, which can be related to $Te^{4+}$ and $Te^{6+}$ species, respectively [30]. However, $Te^{4+}$ cations were present mainly on the surface of the MoVTeCeO catalysts with relatively high V content (e.g., V/Mo = 0.3), whereas $Te^{6+}$ species were seen mainly on the surface of catalysts with relatively low V content (e.g., V/Mo = 0.1). However, $Te^0$ (binding energy of 573.0 eV) was not observed.

The Ce $3d_{5/2}$ peaks of the catalysts could be fitted into two components at 881.8 and 884.8 eV, which can be related to $Ce^{4+}$ and $Ce^{3+}$ ions, respectively [31,32]. Table 1 and Fig. 3 show that $Ce^{3+}$ ions existed mainly in MoVTeCeO catalysts with relatively low V content (e.g., V/Mo = 0.1), whereas $Ce^{4+}$ ions were present mainly in the catalysts with relatively high V content (e.g., V/Mo = 0.3). However, $Ce^{3+}$ ions existed mainly in the Te-free catalyst with relatively high V content (e.g., V/Mo = 0.3). In addition, $Ce^{4+}/Ce^{3+}$ surface atomic ratios decreased slightly with increasing Ce content in the $MoV_{0.3}Te_{0.23}Ce_x$ catalyst system, suggesting that the reduction of $Ce^{4+}$ may have been relatively restrained by the high V content.

### 3.4. $H_2$-TPR studies

The $H_2$-temperature programmed reduction ($H_2$-TPR) profiles and amount of $H_2$ consumption of $MoV_{0.3}Ce_{0.2}$, $MoTe_{0.23}Ce_{0.2}$, $MoV_{0.1}Te_{0.23}Ce_{0.2}$, and $MoV_{0.3}Te_{0.23}Ce_x$ ($x = 0.1-0.3$) are shown in Fig. 4 and Table 2. The $H_2$-TPR profile of the Ce-free sample $MoV_{0.3}Te_{0.23}$ (Fig. 4g) displays three peaks at 652, 710, and 746 °C. According to previous work [33–35], the weak reduction peak observed at 652 °C may be attributed to a stepwise reduction of $V_2O_5 \rightarrow 1/3V_6O_{13}$ and a complex reduction reaction of $MoO_3 \rightarrow MoO_2$ and/or $TeO_2 \rightarrow Te$. The peak at 710 °C could be related to a stepwise reduction of $V_6O_{13} \rightarrow 6VO_2$, whereas the peak at 746 °C could be assigned to a stepwise reduction of $MoO_2 \rightarrow Mo$. When cerium was added into the catalysts at a Ce/Mo ratio of 0.1 or 0.2, for only one peak each appeared for Mo, V, and/or Te in the catalyst. Moreover, the value of $T_{max}$ for the main peak shifted to around 682 °C. Compared with the previous reports [33,34] and our earlier experimental results [35], this peak may not be attributed to the reduction of single Mo, V, Te, or Ce ions (Figs. 4a and 4b). The reduced species may be a crystalline phase (e.g., M1 phase). Consequently, this indicates that in the presence of cerium, there are synergetic effects among the Mo, V, Te, and Ce ions in the reduction procedure. A further increase in cerium content to a Ce/Mo ratio of 0.3 caused the appearance of a peak at around 751 °C, suggesting the reduction of $MoO_2 \rightarrow Mo$.

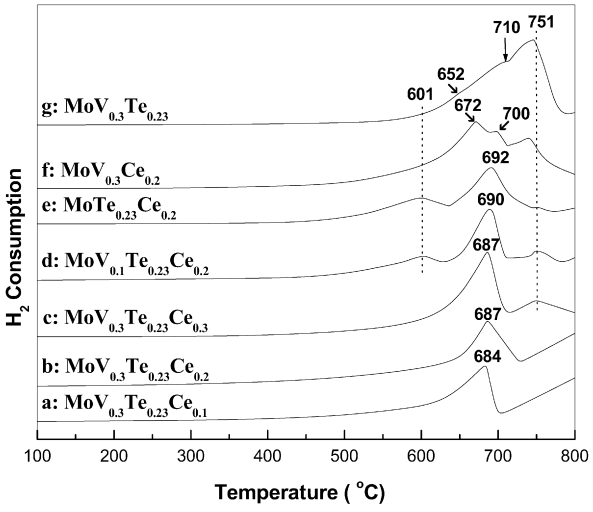


Fig. 4. The $H_2$-TPR profiles of samples calcined at 600 °C in $N_2$.

For the low V-containing or V-free samples (Figs. 4d and 4e), a first TPR peak appeared at about 601 °C, considered to be due to the reduction of the surface-capping oxygen of ceria. A similar result was reported by Yasyerli et al. [36] in a study on $H_2S$ oxidation over a Ce–V catalyst. However, with increasing V content from a V/Mo ratio of 0.1 to 0.3, this peak disappeared and a second peak at around 692 °C shifted to 684 °C for the $MoV_{0.3}Te_{0.23}Ce_{0.1}$ sample. These results indicate that the relative vanadium content in the catalysts can properly modify the catalysts' redox capability.

To estimate the $H_2$ consumption, the area of TPR profile was integrated (Table 2). The $H_2$ consumption was found to increase in the sequence $MoV_{0.3}Te_{0.23}Ce_{0.2} < MoV_{0.3}Te_{0.23}Ce_{0.1} < MoV_{0.1}Te_{0.23}Ce_{0.2} < MoTe_{0.23}Ce_{0.2} < MoV_{0.3}Te_{0.23}Ce_{0.3} < MoV_{0.3}Ce_{0.2} < MoV_{0.3}Te_{0.23}$. Combining these findings with the XPS data (Table 1) demonstrates that the $Mo^{6+}/V^{5+}/Ce^{4+}$ content on the surface of the MoVTeCeO catalysts varies widely; thus, determining which element contributes most to the reduction is difficult. In other words, the results demonstrate that the reducibility of Mo–V–Te–Ce–O catalysts may not be determined by single element in a high-oxidation state (e.g., $Mo^{6+}$, $V^{5+}$, or $Ce^{4+}$) on the catalyst surface. Such behavior seems to be related to changes in the nature of the crystalline phases as well as in the oxidation state of each element.

### 3.5. Catalytic properties

The catalytic results obtained for the oxidation of isobutane over the catalysts at 420 °C, given in Table 3, indicate that all

Table 2
The $H_2$-TPR results of samples calcined at 600 °C in $N_2$

| | Sample | | | | | | |
|---|---|---|---|---|---|---|---|
| | $MoV_{0.3}Te_{0.23}$ | $MoV_{0.3}Ce_{0.2}$ | $MoTe_{0.23}$ $Ce_{0.2}$ | $MoV_{0.1}Te_{0.23}Ce_{0.2}$ | $MoV_{0.3}Te_{0.23}Ce_{0.1}$ | $MoV_{0.3}Te_{0.23}Ce_{0.2}$ | $MoV_{0.3}Te_{0.23}Ce_{0.3}$ |
| Temperature (°C) | 652/710/746 | 672/700/739 | 601/692/751 | 601/690/751 | 684 | 687 | 687/751 |
| Weight (mg) | 10 | 10 | 10 | 10 | 10 | 10 | 10 |
| $H_2$ consumption (μmol) | 13.4/34.5/26.2 | 25.1/12.3/10.7 | 5.6/22.8/0.4 | 3.6/20.0/4.1 | 26.6 | 23.3 | 33.8/6.1 |

Table 3
Catalytic data of the catalysts for isobutane oxidation at 420 °C[a]

| Sample | Conversion (%) | Selectivity (%) | | | | | | |
|---|---|---|---|---|---|---|---|---|
| | $i$-$C_4H_{10}$ | $i$-$C_4^=$ | MAL | MAA | $CO_x$ | $C_3^=$ | HAC | Others[b] |
| $MoV_{0.3}Te_{0.23}$ | 18.8 | 1 | 15 | 11 | 58 | 6 | 8 | 1 |
| $MoV_{0.3}Te_{0.23}Ce_{0.1}$ | 19.5 | 14 | 24 | 15 | 34 | 6 | 4 | 3 |
| $MoV_{0.3}Te_{0.23}Ce_{0.2}$ | 20.2 | 10 | 33 | 20 | 28 | 4 | 2 | 3 |
| $MoV_{0.3}Te_{0.23}Ce_{0.3}$ | 22.7 | 5 | 20 | 10 | 51 | 4 | 8 | 2 |
| $MoV_{0.1}Te_{0.23}Ce_{0.2}$ | 21.6 | 15 | 21 | 7 | 44 | 7 | 4 | 2 |
| $MoTe_{0.23}Ce_{0.2}$ | 23.4 | 17 | 20 | 6 | 43 | 7 | 5 | 2 |
| $MoV_{0.3}Ce_{0.2}$ | 24.5 | 2 | 4 | 9 | 73 | 5 | 6 | 1 |

[a] Reaction condition: GHSV = 3600 ml $h^{-1}$ $g_{cat}^{-1}$, $P = 101$ kPa.
[b] Acetone, acrolein, acrylic acid, etc.

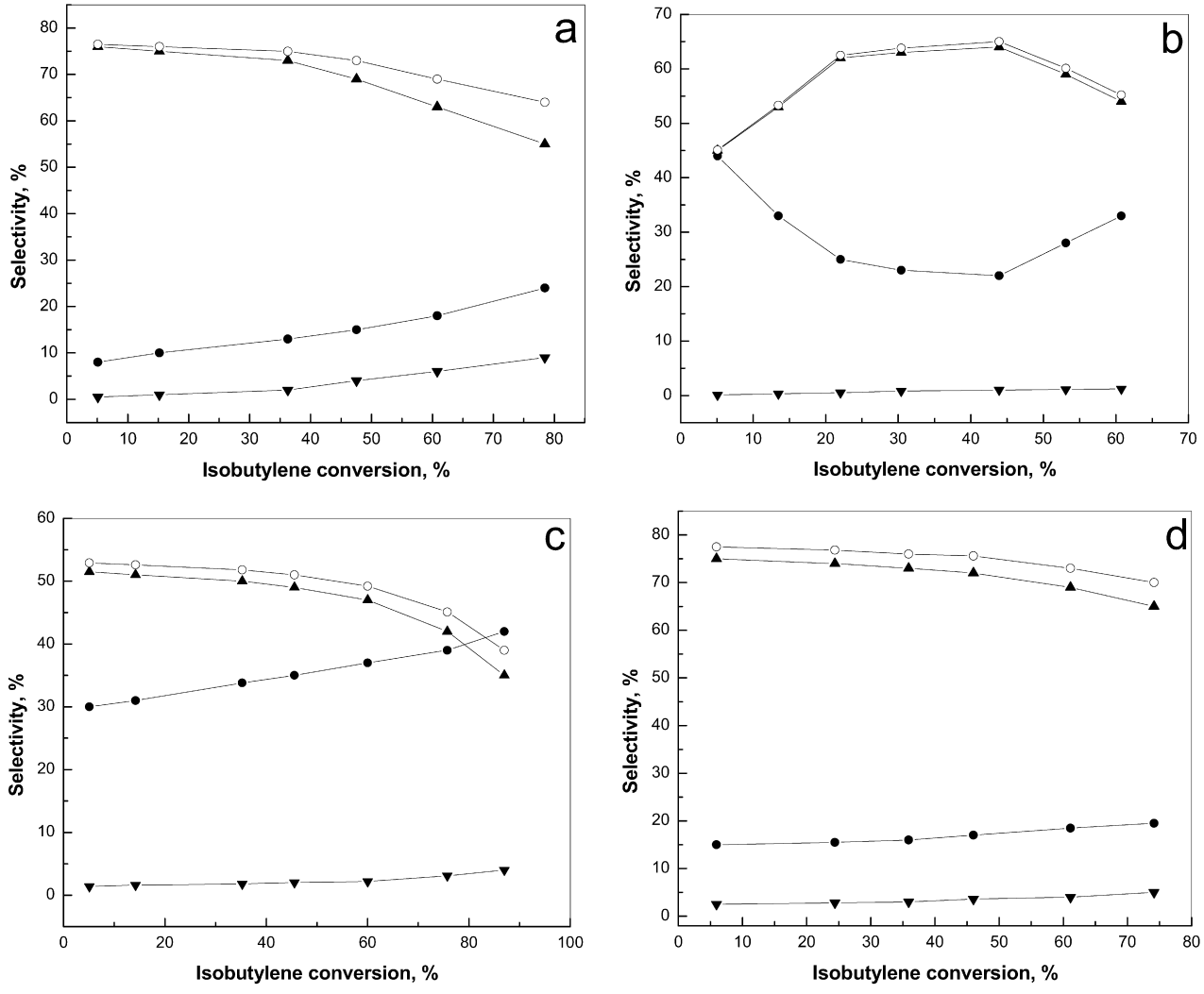


Fig. 5. Variation in the selectivities to the main products of the partial oxidation with the isobutylene conversion obtained during the oxidation of isobutylene at 420 °C over (a) the $MoV_{0.3}Te_{0.23}$ catalyst, (b) the $MoTe_{0.23}Ce_{0.2}$ catalyst, (c) the $MoV_{0.3}Ce_{0.2}$ catalyst, (d) the $MoV_{0.3}Te_{0.23}Ce_{0.2}$ catalyst. Symbols: (▲) MAL, (▼) MAA, (●) $CO_x$, (○) MAL + MAA.

of the Mo–Te-containing catalysts were active and selective for the partial oxidation of isobutane to MAL. Moreover, the selectivity to MAL and MAA was improved considerably by the addition of small amounts of cerium. For example, the selectivity to MAL and MAA reached 24 and 15%, respectively, at Ce/Mo ratios as low as 0.1. The MAL and MAA selectivities increased continuously with increasing cerium content, reaching a maximum (33% MAL selectivity and 20% MAA selectivity) at a Ce/Mo ratio of 0.2. However, the MAL and MAA selectivities decreased with further increases in cerium content.

In addition, clearly the highest selectivity to isobutylene and the lowest selectivity to MAA could be obtained over V-free

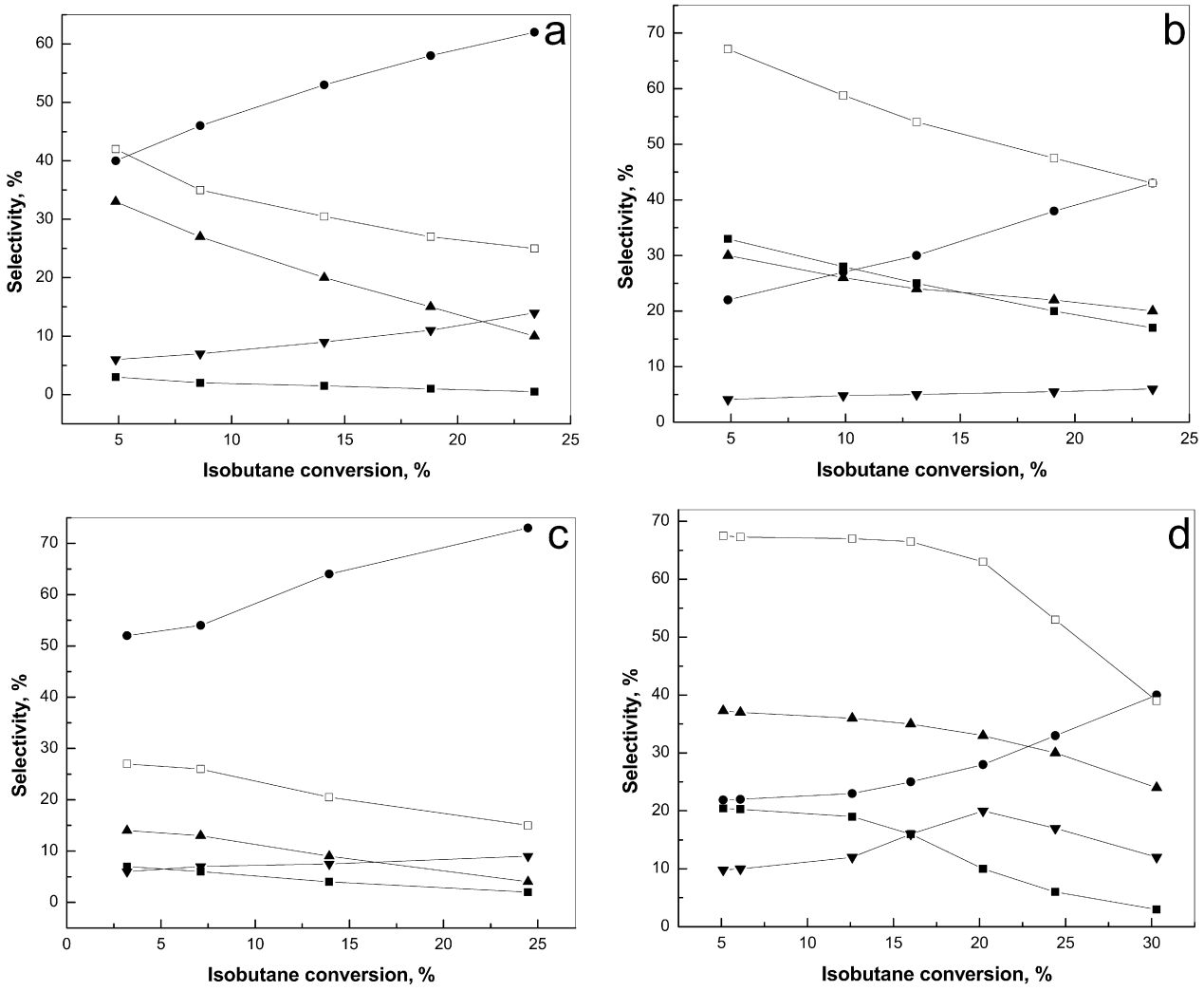


Fig. 6. Variation in the selectivities to the main products of the partial oxidation with the isobutane conversion obtained during the oxidation of isobutane at 420 °C over (a) the $MoV_{0.3}Te_{0.23}$ catalyst, (b) the $MoTe_{0.23}Ce_{0.2}$ catalyst, (c) the $MoV_{0.3}Ce_{0.2}$ catalyst, (d) the $MoV_{0.3}Te_{0.23}Ce_{0.2}$ catalyst. Symbols: (■) isobutylene, (▲) MAL, (▼) MAA, (●) $CO_x$, (□) isobutylene + MAL + MAA.

catalyst $MoTe_{0.23}Ce_{0.2}$. Thus, it can be concluded that the incorporation of vanadium into the Mo–Te–Ce-based system had a positive effect on the transformation of isobutylene to MAA in the selective oxidation of isobutane.

In contrast, the catalytic results given in Table 3 show that the selectivities to MAA over $MoTe_{0.23}Ce_{0.2}$ and $MoV_{0.1}Te_{0.23}Ce_{0.2}$ catalysts, in which Te ions are mainly in a +6 oxidation state on the catalyst surface (Table 1), were lower than those obtained over the $Te^{4+}$-containing $MoV_{0.3}Te_{0.23}Ce_{0.2}$ catalyst. It can be suggested that the presence of $Te^{4+}$ ions in the catalysts favors the formation of MAA. In this way, these results demonstrate that the V–$Te^{4+}$-containing phase (e.g., M1 phase) was active and selective in the selective oxidation of isobutane to MAA.

Fig. 5 shows the variation in selectivities to the main products of the reaction with the isobutylene conversion obtained during the oxidation of isobutylene over the four Mo-based catalysts. It is well known that the primary products of a given reaction can be discriminated from high-order products by extrapolating product selectivity to zero conversion. Primary products have nonzero intercepts, whereas secondary and high-order products have zero intercepts [37]. Therefore, in the case of selective oxidation of isobutylene over $MoV_{0.3}Te_{0.23}Ce_x$ catalysts (Fig. 5), clearly the dominant primary product was MAL, because MAL selectivity increased gradually with decreasing isobutylene conversion.

In the V-free catalyst $MoTe_{0.23}Ce_{0.2}$ (Fig. 5d), MAL selectivity was strongly affected by the reaction gas hourly space velocity. Only when the gas hourly space velocity remained at an optimum value could maximal MAL selectivity and yield be obtained. Thus, it can be concluded that the incorporation of a small amount of V may have a positive effect on the adsorption and activation of isobutylene, which in return improves the selectivity to MAL. However, over the V-containing catalysts, the selectivity to MAA increased and the selectivity to MAL decreased with increasing isobutylene conversion, indicating that MAA may be formed by a consecutive reaction of MAL. Moreover, the addition of Ce into the $MoV_{0.3}Te_{0.23}$-based catalyst enhanced MAL selectivity at relatively high isobutylene conversion. Considering that the $Mo^{6+}/Mo^{5+}$ surface atomic ratio

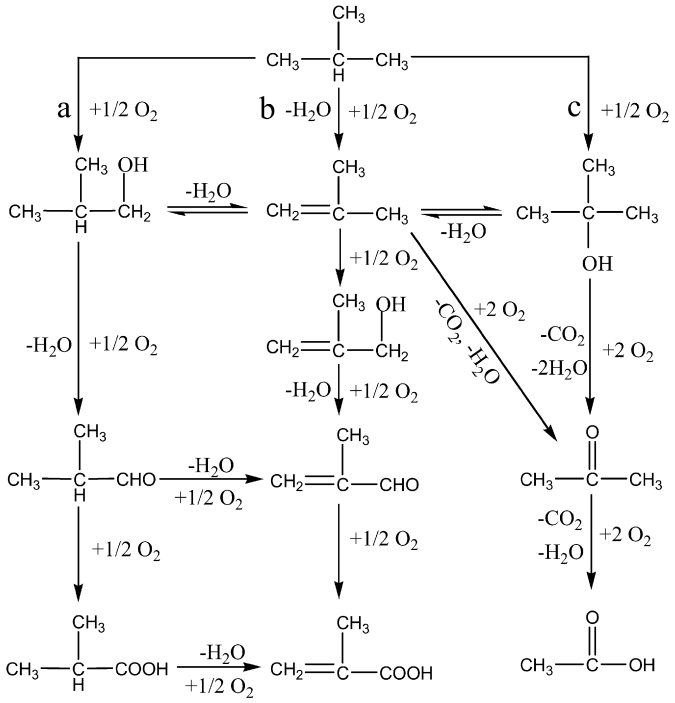


Fig. 7. Reaction scheme for the oxidation of isobutane on MoVTeCeO catalysts.

in the $MoV_{0.3}Te_{0.23}Ce_{0.2}$ catalyst was higher than that in the $MoV_{0.3}Te_{0.23}$ catalyst, it has been suggested that $Mo^{6+}$ species should be involved in the selective O insertion of olefinic intermediate [21,26].

Fig. 6 shows the variation in selectivities to the main reaction products with the isobutane conversion obtained during the oxidation of isobutane over the four Mo-based catalysts. The product distributions were relatively different, depending strongly on the chemical composition of the catalysts. In general, CO and $CO_2$ were the main products. Isobutylene, MAL, and MAA also were main products over the MoVTeCeO catalyst. Of the four catalysts studied, the V-free $MoTe_{0.23}Ce_{0.2}$ catalyst (Fig. 6b) exhibited the highest selectivity to isobutylene and the lowest selectivity to MAA. But when vanadium was added into the Mo–Te-based system (Fig. 6a), the selectivity to isobutylene decreased significantly, whereas the selectivity to MAA increased only relatively. These findings suggest that part of the isobutylene was transformed to MAA over a V-containing phase. Moreover, the incorporation of Ce into the Mo–V–Te-based system also improved the selectivity to MAA in the selective oxidation of isobutane, although it had almost no effect on the selective oxidation of isobutylene. This indicates that the incorporation of Ce can have a positive effect on both activity and selectivity.

In addition, it can be concluded that the selectivity to MAA in the selective oxidation of isobutane over $MoV_{0.3}Te_{0.23}$ (Fig. 6a) and $MoV_{0.3}Te_{0.23}Ce_{0.2}$ (Fig. 6d) catalysts is generally higher than that in the selective oxidation of isobutylene (Figs. 5a and 5d). Based on the foregoing discussion, we can propose that MAA was formed not only from MAL, but also directly from isobutane or an intermediate. A reaction scheme for the selective oxidation of isobutane is given in Fig. 7.

In analogy with the oxidation of propane to acrylic acid [38–42], we propose the following reaction pathway for the oxidation of isobutane (Fig. 7). From isobutane, we can envision at least three possible reaction pathways leading to various partial oxidation products as described in Fig. 7. In path a, iso-butanol is formed by insertion of one oxygen atom into the methyl C–H bond, which dehydrates to isobutylene or is oxidized to MAL and MAA through iso-butyric aldehyde and iso-butyric acid, respectively. Path b is a direct oxidative dehydrogenation from isobutane to isobutylene, followed by oxidation to MAA through MAL. In path c, tert-butanol is formed by insertion of one oxygen atom into the methine C–H bond, which can dehydrate to isobutylene or further oxidize to acetone. As a matter of fact, in the oxidation of isobutane, iso-butanol is obtained in substantial quantities, especially in the case of reaction at relatively low temperature (360–380 °C). This result suggests that path a is very possible. However, we are unable to determine whether pathway c or an iso-butanol intermediate truly exist.

Selective oxidation reactions of alkanes on mixed-oxide catalysts often show similar reaction kinetics, in which the activation of alkanes is generally a rate-determining step. In the heteropolyacid system, Mo is the active site for the selective oxidation of isobutane to MAA [14]. According to our results given in Table 3, Figs. 5 and 6, the V-free catalysts also showed relatively high activity for the reaction compared with the V-containing catalysts. In particular, the relatively low Ce-content V-containing catalysts exhibited good catalytic performance, although no V species were detected on the catalyst surface. Therefore, Mo appears to be a key element in isobutane activation. In other words, the active crystalline phase for the transformation of isobutane to isobutylene should be a Mo-containing phase or a mixture of several phases. However, the effect of V on the isobutane activation cannot be excluded.

It is generally accepted that the presence of TeMo-containing crystalline phase may be a key factor in the selective oxidation of propene to acrolein over MoVTe-based catalysts. Our experimental results lead to a similar conclusion, that isobutylene oxidation to MAL occurs over a TeMo-containing phase. It has been reported that in the selective oxidation of propane over Mo–V–Sb–Nb–O catalyst, the presence of $(M_xMo_{1-x})_5O_{14}$ ($M$ = V or Nb) favors the formation of acrylic and acetic acid [42,43]. This proposal is not supported by our experimental results, however. As mentioned above, we found that the $Te^{4+}$-containing phase (e.g., M1 phase) appears to be a determining factor for the selective oxidation of isobutane to MAA.

According to our experimental results, the role of V is related to the formation of active and/or selective crystalline phases, such as M1, which has been reported to be active for the propene oxidation to acrolein and acrylic acid [20,21] and was found to be active for isobutylene oxidation to MAL in the present study. In addition, the formation of the redox cycle $V^{4+} + Mo^{6+} \rightleftarrows V^{5+} + Mo^{5+}$ may improve the redox capability of Mo species.

It has been reported that Ce has a strong capability for storing oxygen, which can improve the mobility of lattice oxygen in the catalysts. Moreover, Ce can join the redox cycle $Ce^{3+} + Mo^{6+} \rightleftarrows Ce^{4+} + Mo^{5+}$ [44]. In addition, the role of Ce is

related to the formation of active Te$MO$ crystalline phases. It should be noted that the addition of small amounts of Ce to the MoVTe-based catalyst modified this catalyst's reduction to improve the title reaction. Due to these factors, we conclude that the MoVTe-based catalysts with an optimum Ce content may exhibit relatively good activity and selectivity for the selective oxidation of isobutane. In summary, the presence of all four elements—Mo, V, Te, and Ce—is necessary to achieve high selectivities in MAL and MAA.

## 4. Conclusion

The addition of Ce to a MoVTe-based system modified its physicochemical properties (e.g., crystalline phases, reducibility, surface composition, and surroundings of Mo), affecting the system's catalytic performance for the selective oxidation of isobutane to MAL and MAA. Under our reaction conditions, the $MoV_{0.3}Te_{0.23}Ce_{0.2}$ catalyst achieved the best MAL and MAA selectivity (53%) and yield (10.7%) at 420 °C.

## Acknowledgments

This work was supported by the National Basic Research Program of China (2004CB217804) and the National Natural Science Foundation of China (20673046).

## References

[1] M. Misono, N. Nojiri, Appl. Catal. 64 (1990) 1.
[2] R.H. Schwaar, Methacrylic Acid and Esters, Process Economics Program Report No. 11D, SRI International, 1993.
[3] W. Li, W. Ueda, Catal. Lett. 46 (1997) 261.
[4] J.S. Min, N. Mizuno, Catal. Today 66 (2001) 47.
[5] J.H. Holles, C.J. Dillon, J.A. Labinger, M.E. Davis, J. Catal. 218 (2003) 42.
[6] J.S. Paul, J. Urschey, P.A. Jacobs, W.F. Maier, F. Verpoort, J. Catal. 220 (2003) 136.
[7] T. Shishido, A. Inoue, T. Konishi, I. Matsuura, K. Takehira, Catal. Lett. 68 (2000) 215.
[8] H. Liu, E.M. Gaigneaux, H. Imoto, T. Shido, Y. Iwasawa, Appl. Catal. A 202 (2000) 251.
[9] T. Inoue, K. Asakura, W. Li, S.T. Oyama, Y. Iwasawa, Appl. Catal. A 165 (1997) 183.
[10] V. Cortés Corberán, M. Jia, J. El-Haskouri, R.X. Valenzuela, D. Beltrán-Porter, P. Amorós, Catal. Today 91–92 (2004) 127.
[11] J. Guan, M. Jia, S. Jing, Z. Wang, L. Xing, H. Xu, Q. Kan, Catal. Lett. 108 (2006) 125.
[12] J. Guan, S. Wu, M. Jia, J. Huang, S. Jing, H. Xu, Z. Wang, W. Zhu, H. Xing, H. Wang, Q. Kan, Catal. Commun. 8 (2007) 1219.
[13] C. Marchal-Roch, N. Laronze, N. Guillou, A. Tézé, G. Hervé, Appl. Catal. A 199 (2000) 33.
[14] G.P. Schindler, T. Ui, K. Nagai, Appl. Catal. A 206 (2001) 183.
[15] S. Gao, J.B. Moffat, Appl. Catal. A 229 (2002) 245.
[16] F. Cavani, F. Trifirò, Appl. Catal. A 88 (1992) 115.
[17] E. Etienne, F. Cavani, R. Mezzogori, F. Trifirò, G. Calestani, L. Gengembre, M. Guelton, Appl. Catal. A 256 (2003) 275.
[18] C. Leitenburg, A. Trovarelli, J. Llorca, F. Cavani, G. Bini, Appl. Catal. A 139 (1996) 161.
[19] M. Aouine, J.L. Dubois, J.M.M. Millet, Chem. Commun. (2001) 1180.
[20] P. Botella, J.M. López Nieto, B. Solsona, A. Mifsud, F. Márquez, J. Catal. 209 (2002) 445.
[21] R.K. Grasselli, J.D. Burrington, D.J. Buttrey, P. DeSanto Jr., C.G. Lugmair, A.F. Volpe Jr., T. Weingand, Top. Catal. 23 (2003) 5.
[22] T. Ushikubo, K. Oshima, A. Kayou, M. Hatano, Stud. Surf. Sci. Catal. 112 (1997) 473.
[23] I.E. Wachs, Catal. Today 27 (1996) 437.
[24] W.X. Kuang, Y.N. Fan, K.W. Yao, Y. Che, J. Solid State Chem. 140 (1998) 354.
[25] J.C.J. Bart, F. Cariati, A. Sgamelloti, Inorg. Chim. Acta 36 (1979) 105.
[26] P. Botella, P. Concepción, J.M. López Nieto, Y. Moreno, Catal. Today 99 (2005) 51.
[27] Y. Zhu, W. Lu, H. Li, H. Wan, J. Catal. 246 (2007) 382.
[28] J.W. Robinson, Handbook of Spectroscopy, vol. 1, CRC Press, Boca Raton, FL, 1974, p. 615.
[29] M. Demeter, M. Newman, W. Reichelt, Surf. Sci. 454–456 (2000) 41.
[30] H. Hayashi, N. Shigemoto, S. Sugiyama, N. Masaoka, K. Saitoh, Catal. Lett. 19 (1993) 273.
[31] A. Laachir, V. Perrichon, A. Badri, J. Chem. Soc. Faraday Trans. 87 (1991) 1601.
[32] F.L. Normand, L. Hilaire, K. Kili, J. Phys. Chem. 92 (1988) 2561.
[33] I.L. Botto, C.I. Cabello, H.J. Thomas, Mater. Chem. Phys. 47 (1997) 37.
[34] L. Chen, J. Liang, H. Lin, W. Weng, H. Wan, J.C. Védrine, Appl. Catal. A 293 (2005) 49.
[35] J. Guan, G. Wang, S. Jing, Z. Wang, Q. Kan, Polish J. Chem. 80 (2006) 1397.
[36] S. Yasyerli, G. Dogu, T. Dogu, Catal. Today 117 (2006) 271.
[37] J.N. Michaels, D.L. Stern, R.K. Grasselli, Catal. Lett. 42 (1996) 135.
[38] M. Ai, Catal. Today 13 (1992) 679.
[39] M.M. Bettahar, G. Costentin, L. Savary, J.C. Lavalley, Appl. Catal. A Gen. 145 (1996) 1.
[40] M. Lin, T.B. Desai, F.W. Kaiser, P.D. Klugherz, Catal. Today 61 (2000) 223.
[41] M.M. Lin, Appl. Catal. A Gen. 207 (2001) 1.
[42] J.C. Védrine, E.K. Novakova, E.G. Derouane, Catal. Today 81 (2003) 247.
[43] E.K. Novakova, E.G. Derouane, J.C. Védrine, Catal. Lett. 83 (2002) 177.
[44] X. Zhang, H. Wan, W. Weng, X. Yi, J. Mol. Catal. A Chem. 200 (2003) 291.